IEICE TRANSACTIONS

on Communications

VOL. E107-B NO. 1
JANUARY 2024

A PUBLICATION OF THE COMMUNICATIONS SOCIETY

The Institute of Electronics, Information and Communication Engineers
Kikai-Shinko-Kaikan Bldg., 5-8, Shibakoen 3chome, Minato-ku, TOKYO, 105-0011 JAPAN

PAPER

Improvement of Channel Capacity of MIMO Communication Using Yagi–Uda Planar Antennas with a Propagation Path through a PVC Pipe Wall

Akihiko HIRATA[†a)], ***Senior Member***, **Keisuke AKIYAMA**[†], **Shunsuke KABE**[†], ***Nonmembers***, **Hiroshi MURATA**[††], ***and*** **Masato MIZUKAMI**[†††], ***Members***

SUMMARY This study investigates the improvement of the channel capacity of 5-GHz-band multiple-input multiple-output (MIMO) communication using microwave-guided modes propagating along a polyvinyl chloride (PVC) pipe wall for a buried pipe inspection robot. We design a planar Yagi–Uda antenna to reduce transmission losses in communication with PVC pipe walls as propagation paths. Coupling efficiency between the antenna and a PVC pipe is improved by attaching a PVC adapter with the same curvature as the PVC pipe's inner wall to the Yagi–Uda antenna to eliminate any gap between the antenna and the inner wall of the PVC pipe. The use of a planar Yagi–Uda antenna with a PVC adaptor decreases the transmission loss of a 5-GHz-band microwave signal propagating along a 1-m-lomg straight PVC pipe wall by 7 dB compared to a dipole antenna. The channel capacity of a 2×2 MIMO system using planar Yagi–Uda antennas is more than twice that of the system using dipole antennas.
key words: *Yagi–Uda antenna, microwave propagation, MIMO, pipelines*

1. Introduction

Recently, the aging of buried pipes such as water and gas pipes has become a major issue. Demand for efficient and nondestructive buried pipe inspection methods is increasing. Monitoring the interior of narrow buried pipes that are inaccessible to humans using a robot running inside the pipe is a promising solution [1], [2]. To inspect the interior of a buried pipe using a robot, control and sensing signals must communicate with the robot. However, if communication with robots is achieved with a communication cable, it will restrict the movement of robots. If wireless communication is used to communicate with a robot, its movement will not be restricted by a communication cable. Various studies about the wireless communication with a robot running inside the pipe have been reported [3]–[6]. However, when the inner diameter of a pipe is narrow, communication distance is limited due to the propagation loss of microwaves in the pipe [7]–[11].

To solve the issues, we investigated communication methods using microwave-guided modes propagating along the walls of dielectric-buried pipes. Several studies have revealed that a relatively low loss transmission of microwave signals can be achieved with microwave-guided modes, which can propagate along fiberglass-reinforced plastic mortar (FRPM) pipe walls [12]–[15]. We have demonstrated that 2.4 and 5 GHz microwave signals can be transmitted several meters along a pipe when a dipole antenna is placed in the cross section of a dielectric buried pipe made of polyvinyl chloride (PVC) or FRPM [8]. First, we used a commercial dipole antenna widely used in 2.4/5-GHz-band wireless LAN terminal adapters, because we are planning to use 2.4/5-GHz-band wireless LAN to communicate with a buried pipe inspection robot. Additionally, we demonstrated data transmission with microwave-guided modes propagating along a PVC pipe wall [16]. Moreover, we investigated the use of a 2×2 multiple-input multiple-output (MIMO) system to increase the channel capacity of communication systems [8]. MIMO systems have drawn considerable attention because they can increase data rates without expanding a frequency band with multiple antennas at transmitter and receiver sites [17]–[22]. Because dipole antennas have a rotationally symmetric radiation pattern with respect to the antenna axis, many radio waves radiate outside the pipe wall when a dipole antenna is mounted on a section of pipes. Furthermore, it is difficult to stably bond a dipole antenna covered by a rod-shaped cover to the pipe wall at the end face of a buried pipe. Therefore, the use of directional antennas is desirable in order to radiate most of its power into the wall of a buried pipe. Additionally, because a buried pipe inspection robot runs inside buried pipes, an antenna installed on the robot cannot be mounted on the cross section of pipes, and should be pressed at the buried pipe's inner wall. Therefore, a directional planar antenna whose radiation pattern is parallel to the substrate is suitable because it can be set close to the inner wall of the buried pipe.

This study investigated a planar Yagi–Uda antenna appropriate for communication with microwave-guided modes propagating along the PVC pipe walls. We selected the planar Yagi–Uda antenna [23]–[25] as a directional planar antenna whose radiation pattern is parallel to the substrate. The Yagi–Uda antenna is a resonant-type antenna, whose radiation efficiency is higher at resonant frequency than traveling

Manuscript received April 14, 2023.
Manuscript revised July 10, 2023.
Manuscript publicized October 13, 2023.
[†]The authors are with the Dept. of Information and Communication Systems Engineering, Chiba Institute of Technology, Narashino-shi, 275-0016 Japan.
[††]The author is with Graduate School of Engineering, Mie University, Tsu-shi, 514-0001 Japan.
[†††]The author is with Graduate School of Engineering, Muroran Institute of Technology, Muroran-shi, 050-8585 Japan.
a) E-mail: hirata.akihiko@p.chibakoudai.jp
DOI: 10.1587/transcom.2023EBP3061

wave type antenna, such as tapered slot antenna or Vivaldi antenna. However, a planar Yagi–Uda antenna cannot adhere closely to the interior of buried pipe walls with a curved surface. Therefore, we designed a planar Yagi–Uda antenna with an adapter having the same curved surface as that of buried pipes. There have been few studies that investigate the antenna that is used to be pressed at the interior wall of the dielectric pipe for microwave guided mode along pipe wall. In an antenna used in contact with the inner wall of a buried pipe, an antenna structure that generates microwave guided modes along the pipe wall with high efficiency was investigated for the first time in this paper. The planar Yagi–Uda antenna with dielectric adaptor with the same curvature as the dielectric pipe's inner wall is our original structure for improving the transmission characteristics of microwave guided mode along dielectric pipe wall. We evaluated the transmission characteristics of microwave-guided modes propagating along the PVC pipe walls in the case of a planar Yagi–Uda antenna with an adaptor. Additionally, we investigated the channel capacity calculated from the transmission characteristics of a 2 × 2 MIMO communication system.

2. Design of a Planar Yagi–Uda Antenna

Figure 1 shows a schematic of a planar Yagi–Uda antenna. We employed a Rogers RT/duroid 5880 as the substrate for the antenna, and the antenna pattern was made of a 0.018-mm-thick copper thin film. The planar Yagi–Uda antenna comprises a standard parallel stripline-fed driving dipole, three directors, and a rectangular reflector [13]. The size and thickness of the Rogers RT/duroid substrate are 88.8 × 44.4 and 0.78 mm, respectively. The electric conductivity of copper is 5.5×10^7 S/m. The dielectric constant of Rogers RT/duroid 5880 is 2.2, and its tangent delta is 0.0009. Driving dipoles were printed on the bottom and top surfaces of parallel substrates and connected to an SMA connector. The directors were printed on the top surface of a substrate and the reflectors were on the bottom surface of the substrate.

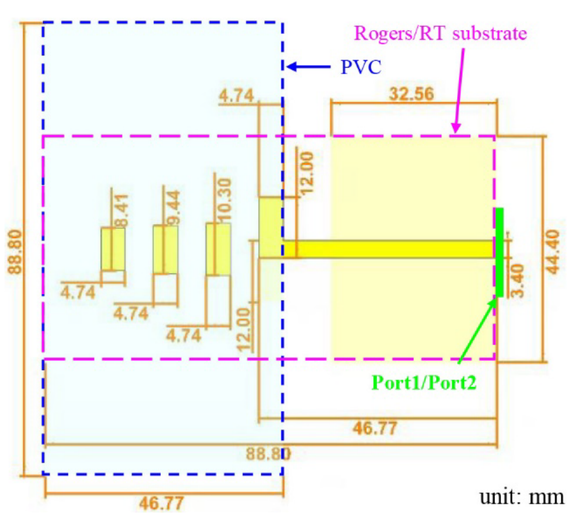

Fig. 1 Schematic of a planar Yagi–Uda antenna.

The planar Yagi–Uda antenna is used for communication using microwave-guided modes propagating along a PVC pipe wall. Therefore, we designed a planar Yagi–Uda antenna with an adapter having the same curved surface as that of the PVC pipe. There are two reasons for the integration of the adapter in the planar Yagi–Uda antenna. The first is to keep the antenna close to the inner wall of the pipe. In order to efficiently direct the microwaves propagating along the pipe wall to the receiving antenna, the receiving antenna should be placed in close contact with the inner wall of the pipe. However, even if the planar Yagi–Uda antenna without the adaptor is pressed against the pipe's inner wall, it is difficult to maintain stable contact with the pipe's inner wall because the antenna is in contact with the inner wall of the pipe only at both edges of the substrate. By using the adapter, the antenna and the inner wall of the PVC pipe contact each other on a plane for stable contact. Another reason is the suppression of reflections at the interface between the PVC pipe wall and the air. Because the surface of the inner wall of PVC pipe is curved, an air layer is formed between the planar Yagi–Uda antenna and the PVC pipe wall in case the PVC adaptor is not attached to the planar Yagi–Uda antenna. In this case, the reflection of 5 GHz band signal at the interface between the PVC pipe wall and the air occurs, which in turn reduces the fraction of 5 GHz band signal that are conducted to the PVC pipe wall. By filling the gap between the PVC pipe wall and the Yagi–Uda antenna with an adapter made of PVC, the 5 GHz band signal can be efficiently conducted to the PVC pipe wall because the discontinuity in dielectric constant between the antenna surface and the PVC pipe wall is eliminated.

To increase transmission efficiency from the antenna to the pipe, the adapter should be made of the same material (PVC) as the pipes. Because antenna impedance changes when an adapter is placed on an antenna substrate, we design an antenna using a model with a 4.5-mm-thick PVC substrate attached to the antenna, as shown in Fig. 1. The dielectric constant of PVC was 3.0, and its tangent delta was 0.02. The length and width of the driving dipole are 12.0 and 4.74 mm, respectively. The length and width of the microstrip line are 46.77 and 3.40 mm, respectively. The distance between the directors was 5.62 mm. The other parameters of the planar Yagi–Uda antenna are shown in Fig. 1. Figures 2(a) and (b) show the images of the top and bottom surfaces of the planar Yagi–Uda antenna substrate, respectively. Figure 2(c) shows an image of the planar Yagi–Uda antenna with a PVC adaptor. To adhere closely to the interior of a pipe with an inner diameter of 130 mm, the adapter was shaped as a cylinder with a diameter of 130 mm cut 4.1 mm thick from the surface of the cylinder. The length of the PVC adaptor is 46.77 mm.

We simulated the S_{11} parameter of the planar Yagi–Uda antenna using a three-dimensional electromagnetic simulator. The simulation results for the S_{11} parameters for antennas with and without PVC adapters are shown in Fig. 3. Port 1 is set at the end of the microstrip line indicated by the green line in Fig. 1. The impedance of a microstrip line

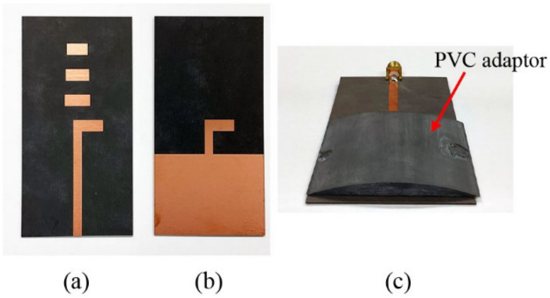

Fig. 2 Images of the (a) top and (b) bottom surfaces of the planar Yagi–Uda antenna substrate (Model B). (c) Image of the planar Yagi–Uda antenna with a PVC adaptor (Model A).

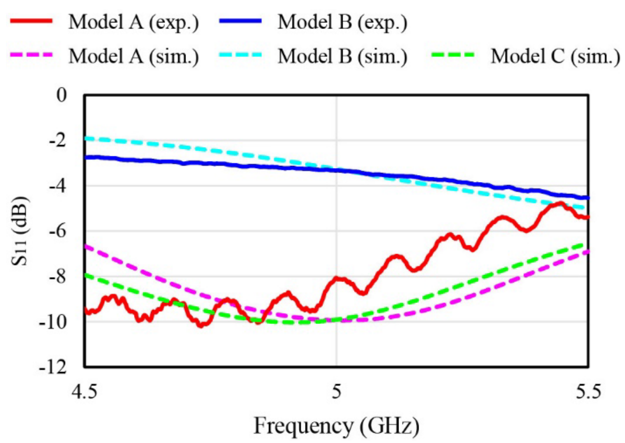

Fig. 3 Simulation and experimental results of S_{11} characteristics of the planar Yagi–Uda antenna with and without a PVC adaptor.

was matched with that of the planar Yagi–Uda antenna with a PVC adapter (Model A), resulting in an S_{11} of −10 dB at 5 GHz. When the PVC adapter was removed from this Yagi–Uda antenna (Model B), the S_{11} was −3.3 dB at 5 GHz because the impedance of the microstrip line is no longer matched to that of the antenna with the PVC adapter. We designed a planar Yagi–Uda antenna without a PVC adaptor whose impedance matching was done at 5 GHz (Model C). The length and width of the driving dipole are 12.4 and 3.0 mm, respectively. The width of the microstrip line is 3.0 mm, and the distance between the directors was 8.9 mm. Simulation results of S_{11} for Model C is also shown in Fig. 3. S_{11} of Model C at 5 GHz was −9.9 dB, therefore, the planar Yagi–Uda antenna without the PVC adaptor in Model C shows good impedance matching at 5.0 GHz.

We measured the S_{11} parameter of the planar Yagi–Uda antenna with a vector network analyzer (VNA). The measurement results are shown in Fig. 3. For the antenna with a PVC adapter, the minimum value of S_{11} is −10 dB, which is consistent with the simulation results. However, the resonant frequency shifts to the lower frequency side by approximately 0.3 GHz. For an antenna without a PVC adapter, the frequency response of S_{11} was generally consistent between experimental and simulated results. Figure 4 shows the simulation results of the radiation pattern of the

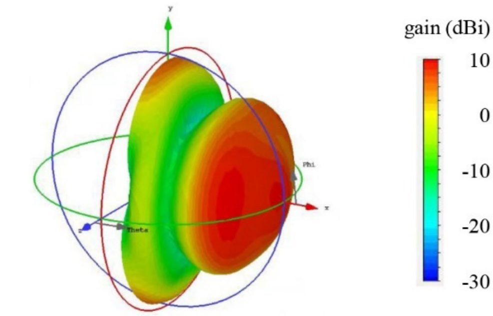

Fig. 4 Simulation results of the radiation pattern of the planar Yagi–Uda antenna with a PVC adaptor (Model A).

planar Yagi–Uda antenna with the PVC adaptor. Most of the power radiated toward the directors, and the simulated gain of the planar Yagi–Uda antenna was 7.7 dBi. These results indicate that the designed planar Yagi–Uda antenna operates directionally at 5 GHz.

3. Propagation Characteristics of Microwave Signals along the Pipe Wall

We investigated the propagation characteristics of a 5-GHz-band microwave signal propagating along the pipe wall of PVC pipes in the case of a Yagi–Uda antenna. Figure 5 shows the simulation results of the electric field distribution along the 0.5-m-long straight PVC pipe for (a) dipole antennas (Model D), (b) planar Yagi–Uda antennas without a PVC adaptor (Model C), and (c) planar Yagi–Uda antennas with a PVC adaptor (Model A). The inner and outer diameters of the PVC pipes are 125 and 140 mm, respectively. In the simulation model, the inside and outside of the pipe are set to air. The boundary conditions of the simulation model are set to perfectly matched layer (PML) boundary. The Port 1 and Port 2 is set at the end of the microstrip line of the planar Yagi–Uda antennas that are set at the both ends of the PVC pipe.

The simulation model and images of the dipole antenna (Model D) are shown in Figs. 6(a) and (b), respectively. The dipole antenna was a dual-band antenna for 2.4 and 5 GHz band wireless LAN, and the length of the dipole antenna for the 5 GHz band was 11 mm. When a dipole antenna was employed, 5-GHz-band microwave signals were circularly radiated symmetrically from the dipole antenna, and the majority of the radiated microwave signals did not propagate along the PVC pipe wall. Microwave signals radiating from the dipole antenna toward the PVC pipe propagated along the PVC pipe wall rather than inside the PVC pipe because the dielectric constant of PVC is higher than that of air. When the planar Yagi–Uda antenna without a PVC adaptor (Model C) was employed, most microwave signals radiated toward the PVC pipe. The electric field strength along the PVC pipe wall for Model C is larger than that for the dipole antenna (Model D), however it is smaller than that for the planar Yagi–Uda antenna with a PVC adaptor (Model A). We suppose that the gap between the inner wall of the PVC pipe and

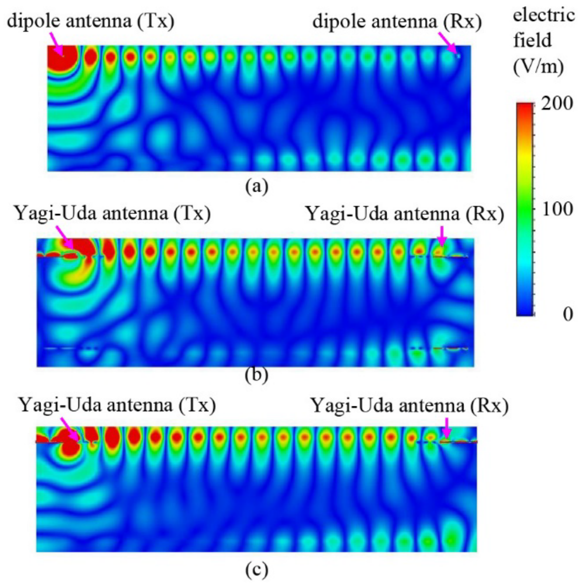

Fig. 5 Simulation results of electric field distribution along a 0.5-m-long straight PVC pipe for the cases of (a) dipole antennas (Model D), (b) planar Yagi–Uda antennas without a PVC adaptor (Model C), and (c) planar Yagi–Uda antennas with a PVC adaptor (Model A).

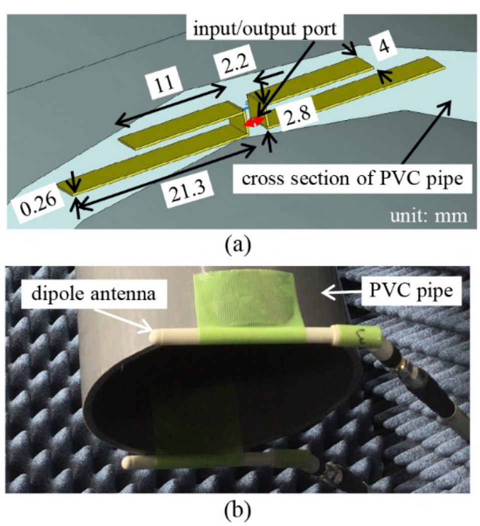

Fig. 6 (a) Simulation model of the dipole antenna attached to the cross-section of the PVC pipe. (b) Image of the dipole antenna attached to the cross section of the PVC pipe.

the planar Yagi–Uda antenna substrate causes the reflection of the 5-GHz-band microwave signal in case a PVC adaptor was not attached with the planar Yagi–Uda antenna.

Figure 7 shows the simulation results of the S_{21} characteristics of microwave-guided modes propagating along the 1-m-long straight PVC pipe in the case of dipole antennas (Model D); planar Yagi–Uda antennas with (Model A) and without a PVC adaptor (Model B and C) were employed. When the dipole antenna was used (Model D), S_{21} dropped significantly below 4.7 GHz because of the frequency characteristics of the antenna itself, and the frequency characteristics of S_{21} were practically constant above 4.8 GHz. S_{21} at 5 GHz is −25.5 dB. The S_{21} characteristics are improved compared to those of the dipole antennas using planar Yagi–Uda antennas. S_{21} at 5 GHz is −20.7 dB (Model B) and −22.0 dB (Model C) for the planar Yagi–Uda antenna without a PVC adaptor, and it is −15.7 dB for the planar Yagi–Uda antenna with a PVC adaptor (Model A). The results indicated that the use of the planar Yagi–Uda antenna with a PVC adaptor decreased the transmission loss of the microwave signal propagating along the PVC pipe wall by 10 dB compared to the dipole antenna.

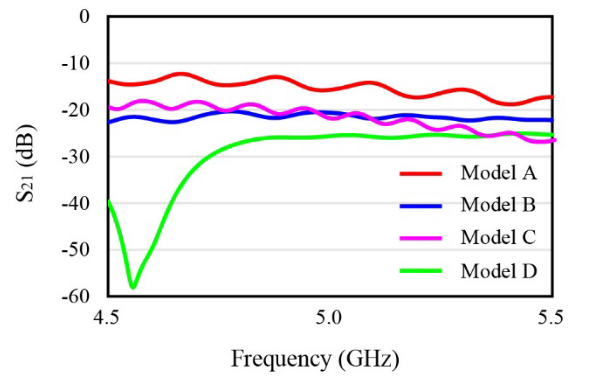

Fig. 7 Simulation results of the S_{21} characteristics of microwave guided-modes propagating along a 1-m-long straight PVC pipe.

Additionally, we measured the S_{21} characteristics of microwave-guided modes propagating along a 1-m-long straight PVC pipe in the case of dipole antennas (Model D), planar Yagi–Uda antennas without a PVC adaptor (Model B), and planar Yagi–Uda antennas with a PVC adaptor (Model A) by VNA. In the experiment, Port 1 and Port 2 are set at the SMA connector. We employed edge mount SMA connector to connect the microstrip line in the planar Yagi–Uda antenna with the SMA cable. The insertion loss of the edge mount SMA connector is estimated to be 0.04 dB at 18 GHz, therefore, the insertion loss of the edge mount SMA connector is negligible. Figures 6(b) and 8 show the images of the dipole antenna and planar Yagi–Uda antenna with a PVC adaptor, respectively. Dipole antennas are mounted on a section of the PVC pipe such that the driving dipole is parallel to the tangent line of the circle. For the planar Yagi–Uda antenna, the tip of the antenna was inserted into the PVC pipe. The PVC adapter attached to the back of the Yagi–Uda antenna ensured that no gap was present between the antenna and the inner wall of the PVC pipe. The PVC pipe is placed on a foamed styrol stand so that it does not touch the desk, and is surrounded by radio wave absorbers.

Figure 9 shows the measurement results of the S_{21} characteristics of the microwave-guided modes propagating along a 1-m-long straight PVC pipe. The S_{21} characteristics were measured using a VNA. The measured S_{21} characteristics of the planar Yagi–Uda antenna with and without a PVC adaptor were practically the same as the simulation results shown in Fig. 7. However, the measured S_{21} characteristics of the dipole antenna are approximately 3 dB higher than

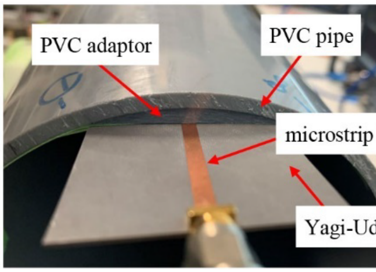

Fig. 8 Image of a planar Yagi–Uda antenna with a PVC adaptor attached to a PVC pipe.

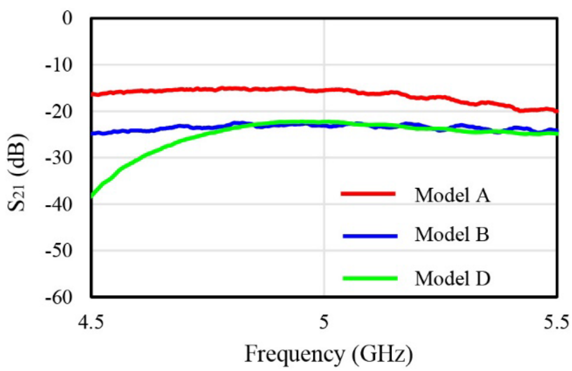

Fig. 9 Experimental results of the S_{21} characteristics of microwave guided-modes propagating along a 1-m-long straight PVC pipe.

the simulation results shown in Fig. 7. The measured S_{21} is −22.5, −23.1, and −15.5 dB for the dipole antenna (Model D), planar Yagi–Uda antenna without a PVC adaptor (Model B), and planar Yagi–Uda antenna with a PVC adaptor (Model A), respectively. The results indicate that the use of the planar Yagi–Uda antenna with a PVC adaptor decreased the transmission loss of the microwave signal propagating along the PVC pipe wall by 7 dB compared to the dipole antenna.

4. MIMO Channel Capacity

MIMO systems generally provide high spectral efficiency and increased capacity using multiple antennas for transmitters and receivers. We have investigated different methods to increase the channel capacity of communication using microwave-guided mode along PVC pipe walls by applying an MIMO system. In this section, we consider the relationship between MIMO channel capacity and antenna type. If the numbers of transmitting and receiving antennas are M and N, respectively, the channel matrix H is calculated by the following equation:

$$H = \begin{pmatrix} h_{11} & \cdots & h_{1M} \\ \vdots & \ddots & \vdots \\ h_{N1} & \cdots & h_{NM} \end{pmatrix} \tag{1}$$

The channel capacity C in MIMO channels is obtained using the following equation [26], [27]:

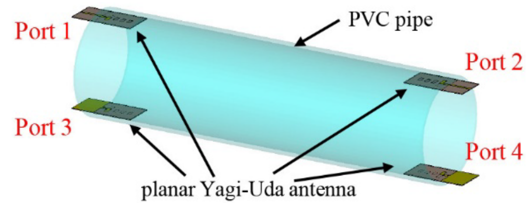

Fig. 10 Experimental results of the S_{21} characteristics of microwave guided-modes propagating along a 0.5-m-long straight PVC pipe.

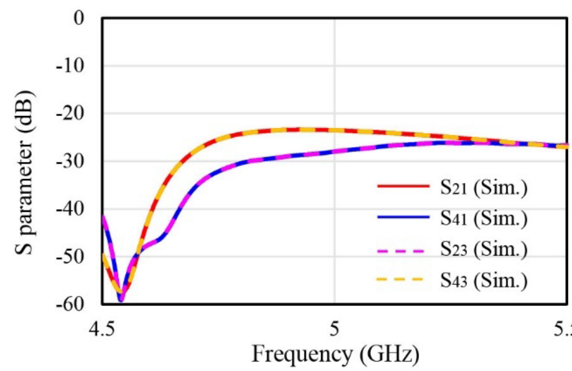

Fig. 11 Simulation results of S parameter of a 2 × 2 MIMO communication system along a 1-m-long straight PVC pipe for the case in which the dipole antennas (Model D) are employed.

$$C = log_2 \left(det \left[I + \frac{P_s}{\sigma^2 M} HH^H \right] \right) \tag{2}$$

$$= \sum_{l=1}^{L} log_2 \left(1 + \frac{P_s \lambda_l}{\sigma^2 M} \right) \tag{3}$$

where P_s and σ^2 denote the transmit power and power of additive complex Gaussian noise, respectively. λ represents the eigenvalue, which is obtained by the matrix of HH^H. L represents the minimum value of N and M.

First, we simulated the channel matrix of a 2×2 MIMO communication system using a simulation model with two antennas at each end of a PVC pipe. Figure 10 shows the simulation model of a 2 × 2 MIMO communication system. On one end of the face of the PVC pipe, two antennas were placed at 180°-rotated positions along the pipe wall. At the other end of the face, the two antennas were installed at the same angular position. Figure 10 shows the simulation model for the channel matrix of the 2 × 2 MIMO communication system with a 0.5-m-long PVC pipe.

Figure 11 shows the simulation results of the S-parameter of the 2×2 MIMO communication system (Model D) along the 1-m-long straight PVC pipe when dipole antennas were employed. Because the simulated PVC pipe was circularly symmetric about its axis, S_{21}, S_{43}, S_{23}, and S_{41} had the same values. S_{23} and S_{41} are −28.0 dB at 5 GHz, and this is 4.5 dB smaller than those of S_{21} and S_{43}. Figure 12 shows the simulation results of the S parameter of the 2 × 2 MIMO communication system along the 1-m-long PVC pipe when the planar Yagi–Uda antennas with a PVC adaptor (Model A) are employed. S_{23} and S_{41} are −15.3 dB at 5 GHz and

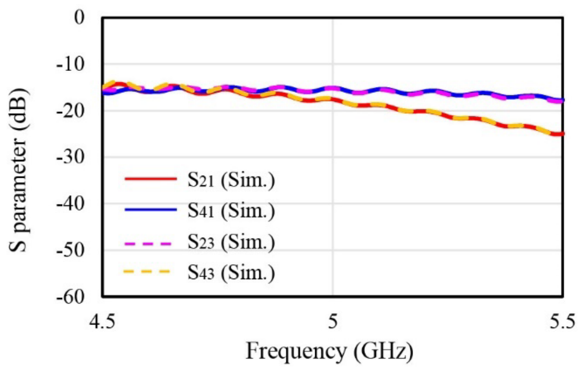

Fig. 12 Simulation results of S parameter of a 2 × 2 MIMO communication system along a 1-m-long straight PVC pipe for the case in which the planar Yagi–Uda antennas with PVC adaptor (Model A) are employed.

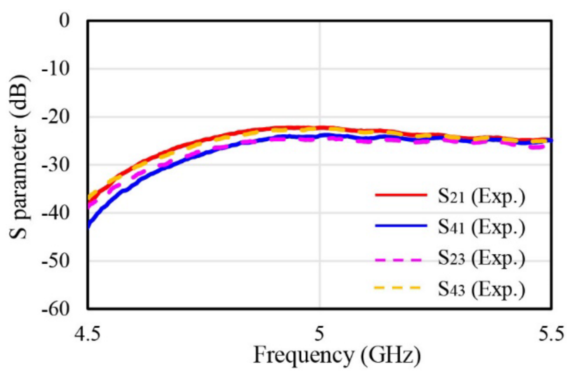

Fig. 13 Experimental results of S parameter of a 2 × 2 MIMO communication system along a 1-m-long straight PVC pipe for the case in which the dipole antennas are employed.

this is 1.5 dB larger than those of S_{21} and S_{43}. Thus, all S-parameters of the 2×2 MIMO communication system with the planar Yagi–Uda antenna with a PVC adaptor are larger than those of the dipole antenna.

Additionally, we measured the channel matrix of a 2×2 MIMO communication system using a four-port VNA. Figures 13 and 14 show the measurement results of the S-parameter of the 2×2 MIMO communication system along the 1-m-long straight PVC pipe when dipole antennas (Model D) and planar Yagi–Uda antennas with a PVC adaptor (Model A) were employed, respectively. The experimental results for the S-parameters obtained for both antennas are in close agreement with the simulation results shown in Figs. 11 and 12. In the case of the dipole antenna (Model D), S_{21}, S_{41}, S_{23}, and S_{43} at 5 GHz are −22.3, −24.0, −24.7, and −22.4 dB, respectively. When the planar Yagi–Uda antenna with a PVC adaptor (Model A) was employed, S_{21}, S_{41}, S_{23}, and S_{43} at 5 GHz are −15.5, −16.4, −16.2, and −15.4 dB, respectively. The experimental results show that the S-parameters of the 2×2 MIMO communication system with planar Yagi–Uda antennas and PVC adapters are greater than those with dipole antennas.

Buried pipes include bent pipes as well as straight pipes. Therefore, we measured the S-parameters of the 2×2 MIMO

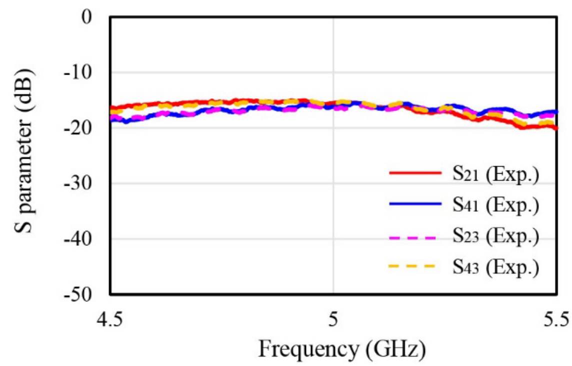

Fig. 14 Experimental results of S parameter of a 2 × 2 MIMO communication system along a 1-m-long straight PVC pipe for the case in which the planar Yagi–Uda antennas with PVC adaptor are employed.

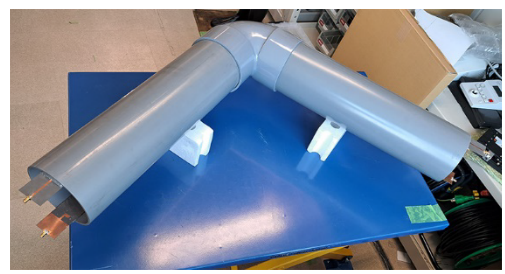

Fig. 15 Photograph of 1-m-long bent PVC pipe with which planar Yagi–Uda antennas are attached.

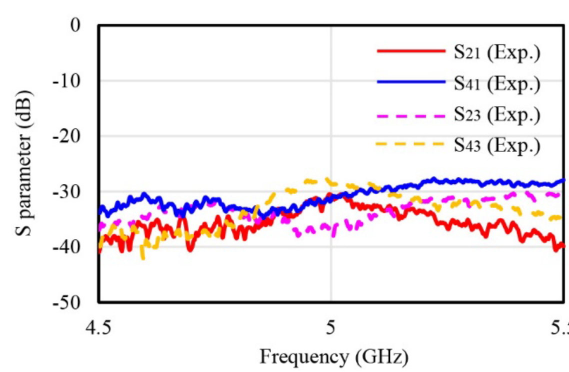

Fig. 16 Experimental results of S parameter of a 2 × 2 MIMO communication system along a 1-m-long bent PVC pipe shown in Fig. 15 for the case in which the planar Yagi–Uda antennas with PVC adaptor (Model A) are employed.

communication system along the 1-m-long bent PVC pipe by VNA. Figure 15 shows the photograph of the 1-m-long bent PVC pipe. Two 0.5-m-long PVC pipes were connected with a 90° bend joint. Figure 16 shows the measured S parameters of the 1-m-long bent PVC pipe in case the planar Yagi–Uda antennas with PVC adaptor (Model A) are employed. The measured S parameters of 1-m-long bent PVC pipe are 12–18 dB smaller than that of 1-m-long straight PVC pipe shown in Fig. 13. We suppose that the reflection loss at the joints and the radiation loss at the 90° bend are responsible for the increased transmission losses along the bent PVC pipe.

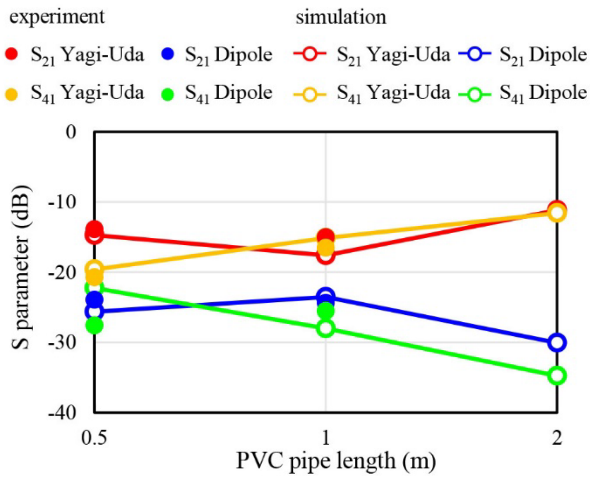

Fig. 17 Simulation and experimental results of dependence of S parameters on straight PVC pipe length.

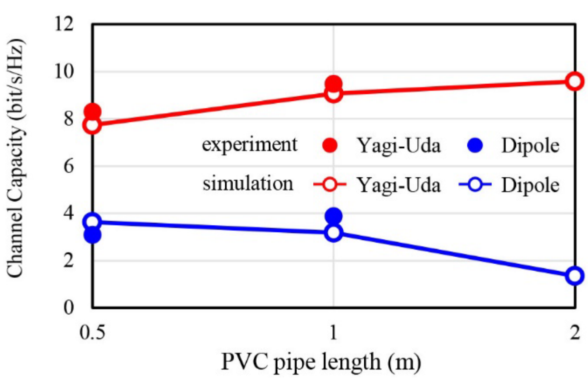

Fig. 18 Simulation and experimental results of dependence of MIMO channel capacity on straight PVC pipe length.

Figure 17 shows the simulation results for the S-parameters as a function of straight PVC pipe length. In the case of the dipole antenna (Model D), both S_{21} and S_{41} are significantly reduced from approximately −25 dB to −35 dB as the length of the PVC pipe is increased from 0.5 to 2 m. In contrast, when the Yagi–Uda antenna was used, increasing the pipe length from 0.5 m to 2 m did not cause a sharp decrease as in the dipole antenna. When the PVC pipe length is over 1 m, S_{21} and S_{41} were approximately 10 dB higher when the Yagi–Uda antenna was used than when the dipole antenna was used. The measured S_{21} and S_{41} for both antennas are shown in Fig. 15. In the experiment, only a 1-m-long PVC pipe could be measured owing to the limited cable length of the VNA. Simulation and experimental results are in general agreement.

Finally, we calculated the channel capacity of the 2×2 MIMO communication system using Eq. (3). P_s/σ^2 is set to be 1000. Figure 18 shows the dependence of MIMO channel capacity on the straight PVC pipe length. For the dipole antenna, the channel capacity was 3.9 bit/s/Hz when the straight PVC pipe length was 1.0 m. It becomes 9.5 bit/s/Hz in case the planar Yagi–Uda antenna with a PVC adaptor is employed. We also calculated the channel capacity of the 2×2 MIMO communication system along 1-m-long bent PVC pipe from the measurement results of S parameters shown in Fig. 16. The calculated channel capacity of the 2×2 MIMO communication system along 1-m-long bent PVC pipe was 0.22 bits/Hz. These results indicate that the use of planar Yagi–Uda antennas with a PVC adaptor increased the channel capacity of the MIMO system compared to the dipole antennas. Moreover, the channel capacity of the 2×2 MIMO communication system along 1-m-long bent PVC pipe becomes approximately 1/43 compared with that along 1-m-long straight PVC pipe.

5. Conclusion

A 5-GHz band planar Yagi–Uda antenna appropriate for communication using microwave-guided modes propagating along a PVC pipe wall was investigated. The coupling efficiency between the antenna and the PVC pipe was improved by attaching a PVC adapter with the same curvature as the inner wall of the PVC pipe to the Yagi–Uda antenna such that no gap remained between the inner wall of the PVC pipe and the antenna. The transmission loss of the 5-GHz microwave signal propagating along the 1-m-lomg straight PVC pipe wall was reduced by 7 dB compared to that of a dipole antenna. The planar Yagi–Uda antenna with a PVC adaptor achieved a MIMO channel capacity of 9.5 bits/s/Hz for a 1.0-m-long straight PVC pipe, which is more than twice that of a MIMO system using a dipole antenna.

Acknowledgments

This study was partially supported by MEXT KAKENHI (Grant Number: JP 21H01328).

References

[1] S. Mikami, M. Mizukami, N.o Hanajima, and Y. Fujihira, "Miniaturized omni-directional mobile mechanism for pipe inspection robots operating in a small and narrow space," Proc. 8th Int. Conf. Asian Society for Precision Engineering and Nanotechnology (ASPEN 2019), C200021, 2019.

[2] T. Kosakai, Y. Kataoka, Y. Ebina, M. Mizukami, and S. Mochizuki, "Two-dimensional self-localization using sensor-fusion of mobile robot for inspecting underground infrastructure facilities," 19th Int. Conf. Precision Engineering, C014, 2022.

[3] H. Ogai, K. Wada, K. Hirai, T. Abe, and G. Sato, "Wireless radio communication system for a pipe inspection robot," 2007 International Conference on Control, Automation and Systems, pp.2616–2619, 2007.

[4] D. Wu, H. Ogai, Y. Yeh, K. Hirai, T. Abe, and G. Sato, "Drain pipe inspection robot using wireless communication system," 2009 ICCAS-SICE, pp.3667–3671, 2009.

[5] J. Akafua, R. Chapman, and H. Guo, "A design of wireless communication and wireless energy transfer system for in-pipe robots," 2021 IEEE Int. Conf. on Wireless for Space and Extreme Environments (WiSEE), pp.84–89, 2021.

[6] J.J. Park, J.W. Moon, H. Kim, S.C. Jang, D.G. Kim, K. Ahn, S.M. Ryew, H. Moon, and H.R. Choi, "Development of the untethered in-pipe inspection robot for natural gas pipelines," 2013 10th Int. Conf. on Ubiquitous Robots and Ambient Intelligence (URAI), pp.55–58,

2013.
[7] V. Doychinov and I.D. Robertson, "Radio wave propagation inside buried sewer pipes for infrastructure robotics," 2021 51st European Microwave Conference (EuMC), 2022, pp.982–985, 2022.
[8] M. Suzuki, K. Fukazawa, A. Hirata, H. Murata, and M. Mizukami, "Study on MIMO communication using microwave guided-modes propagating along PVC pipe wall," 2022 IEEE International Workshop on Electromagnetics: Applications and Student Innovation Competition (iWEM2022), POS1.24, 2022.
[9] I. Sato, N. Shinohara, and D. Jodoi, "Basic study for wireless power transfer to a pipeline inspection robot," 2018 IEEE Wireless Power Transfer Conference (WPTC), pp.1–4, 2018.
[10] G. Harutyunyan, K. Blau, M. Hein, and G. Fuchs, "Wireless signal transmission through non-metallic pipes with transmission gain," 33rd European Microwave Conference Proceedings (IEEE Cat. no.03EX723C), Munich, Germany, vol.2, pp.743–746, 2003, doi: 10.1109/EUMC.2003.177583.
[11] I.F. Akyildiz and E.P. Stuntebeck, "Wireless underground sensor networks: Research challenges," Ad Hoc Networks, vol.4, no.6, pp.669–686, 2006.
[12] K. Yoshida, S. Matsukawa, T. Okuda, M. Hazama, S. Kurokawa, and H. Murata, "Microwave time-domain analysis for non-destructive inspection of FRPM pipelines using electro-optic sensor," 2020 International Topical Meeting on Microwave Photonics (MWP), pp.260–263, 2020.
[13] T. Okuda, K. Katagiri, Y. Otagaki, and H. Murata, "Non-destructive diagnosis of FRPM pipelines using microwave guided-mode and optical fiber link," 2022 Asia-Pacific Microwave Conference (APMC), pp.647–649, 2022.
[14] S. Matsukawa, K. Yoshida, T. Okuda, M. Hazama, S. Kurokawa, and H. Murata, "Non-destructive inspection method for FRPM pipelines utilising time-domain responses of microwave guided-modes," Electronics Letters, vol.56, no.19, pp.982–985, 2020.
[15] S. Matsukawa, K. Yoshida, T. Okuda, M. Hazama, S. Kurokawa, and H. Murata, "Non-destructive inspection for FRPM pipeline using periodic pattern of microwave guided-modes on cylindrical dielectric waveguide," Electronics Letters, vol.57, no.24, pp.933–935, 2021.
[16] T. Noma, Y. Otagaki, H. Murata, A. Hirata, and M. Mizukami, "Video image transfer using microwave guided-modes propagating along PVC pipe-wall," 2022 IEICE General Conference, C-14-5, 2022 (in Japanese).
[17] G.J. Foschini and M.J. Gans, "On limits of wireless communications in a fading environment when using multiple antennas," Wireless Pers. Commun., vol.6, no.3, pp.311–335, 1998.
[18] E.G. Larsson, O. Edfors, F. Tufvesson, and T.L. Marzetta, "Massive MIMO for next generation wireless systems," IEEE Commun. Mag., vol.52, no.2, pp.186–195, 2014.
[19] O.E. Ayach, S. Rajagopal, S. Abu-Surra, Z. Pi and R.W. Heath, "Spatially sparse precoding in millimeter wave MIMO systems," IEEE Trans. Wireless Commun., vol.13, no.3, pp.1499–1513, 2014.
[20] L. Lu, G.Y. Li, A.L. Swindlehurst, A. Ashikhmin, and R. Zhang, "An overview of massive MIMO: Benefits and challenges," IEEE J. Sel. Topics Signal Process., vol.8, no.5, pp.742–758, Oct. 2014.
[21] M.Y. Ali, T. Hossain, and M.M. Mowla, "A trade-off between energy and spectral efficiency in massive MIMO 5G system," 2019 Int. Conf. on Electrical, Computer & Telecomm. Eng. (ICECTE), pp.209–212, 2019.
[22] S. Mohanty, A. Agarwal, S. Mali, G. Misra, and K. Agarwal, "Design and BER performance analysis of MIMO and massive MIMO networks under perfect and imperfect CSI," 2020 Int. Conf. on I-SMAC (I-SMAC), pp.307–312, 2020.
[23] J. Xue, Y. Liu, W. Wang, and H. Liu, "A novel broadband bionic Yagi-Uda antenna with low radar cross section," IET International Radar Conference 2013, pp.1–4, 2013.
[24] Y. Gao, M.T. Ghasr, and R. Zoughi, "Design of a planar wideband Yagi-Uda antenna for millimeter Wave SAR imaging application," 2019 IEEE Int. Symp. on Antennas and Propa. and USNC-URSI 2019, pp.281–282, 2019.
[25] R.A. Alhalabi and G.M. Rebeiz, "Differentially-fed millimeter-wave Yagi-Uda antennas with folded dipole feed," IEEE Trans. Antennas Propag., vol.58, no.3, pp.966–969, 2010.
[26] A. Paulraj, R. Nabar, and D. Gore, Introduction to Space-Time Wireless Communications, Cambridge University Press, Cambridge, UK, 2003.
[27] I.E. Telatar, "Capacity of multiantenna Gaussian channels," Eur. Trans. Telecommun., vol.1, no.6, pp.585–595, Nov./Dec. 1999.

Akihiko Hirata received the B.S. and M.S. degrees in chemistry, and the Dr. Eng. degree in electrical and electronics engineering from Tokyo University, Tokyo, Japan, in 1992, 1994, and 2007, respectively. He joined the Atsugi Electrical Communications Laboratories of Nippon Telegraph and Telephone Corporation (presently NTT Device Technology Laboratories) in Kanagawa, Japan, in 1994. He was a senior research engineer and supervisor at NTT Device Technology Laboratories. Since 2016, he has been a professor at Chiba Institute of Technology. His current research involves millimeter-wave antennas and ultra-broadband millimeter-wave wireless systems. Prof. Hirata is a senior member of the IEEE and a senior member of the IEICE.

Keisuke Akiyama received the B.S. degree in engineering from the Information and Communication Systems Engineering Department, Chiba Institute of Technology, in 2023.

Shunsuke Kabe received the B.S. degree in engineering from the Information and Communication Systems Engineering Department, Chiba Institute of Technology, in 2023.

Hiroshi Murata received the B.Eng., M.Eng., and D.Eng. degrees in electrical engineering from Osaka University in 1988, 1990, and 1998, respectively, for studies on analyses on nonlinear-optic guided-wave systems and its applications to all-optical devices. In 1991, he joined the Department of Electrical Engineering, Faculty of Engineering Science, Osaka University, where he was an Associate Professor in the Division of Advanced Electronics and Optical Science until the end of March 2018. In 2018, he joined the Graduate School Engineering, Mie University, Mie, Japan, where he is currently a Professor. His research is concerned with electro-optics, integrated optics, nonlinear optics and microwave-wave photonics. Dr. Murata is a member of the Institute of Electrical and Electronics Engineers (IEEE), The Optical Society (OSA), the European Microwave Association (EuMA), the Japan Society of Applied Physics, the Optical Society of Japan (OSJ), the Institute of Laser Engineering, and the Institute of Electronics, Information and Communication Engineers (IEICE).

Masato Mizukami received the B.S., M.S. and Dr.Eng. degrees in precision engineering from Kanazawa University, Ishikawa, Japan, in 1988, 1990 and 1997, respectively. He joined Nippon Telegraph and Telephone Corporation, Tokyo, Japan, in 1990, where he was engaged in research on the automated assembly system of opto-mechatronics devices and MEMS. He is currently a professor with the Graduate School of Engineering, Muroran Institute of Technology, Hokkaido, Japan. He is a member of the Robotics Society of Japan and the Japan Society of Mechanical Engineering.